Comparative Analysis of Space Vector Pulse-Width Modulation and Third Harmonic Injected Modulation on Industrial Drives.

C.O. Omeje*; D.B. Nnadi; and C.I. Odeh

Department of Electrical Engineering, University of Nigeria, Nsukka, Nigeria.

E-mail: omejecrescent@yahoo.com*
nnadidamian@yahoo.com

Telephone: +2348069335370

ABSTRACT

This paper presents a detailed analysis of the comparative advantage of space vector pulse width modulation (SVPWM) over the existing third order harmonic injected pulse width modulation. The MATLAB/SIMULINK simulation results obtained from the direct application of 3-level voltage source inverter using SVPWM and third harmonic injected modulation drive strategy on 10 Horse Power, 400 volts,50Hz induction motor are also presented in this work with values of their respective total harmonic distortions been compared. The analysis and results obtained from this work will be very useful in the study of multi-level pulse-width modulation based technique especially in the industrial drive applications. This work will also help in determining the most efficient modulation strategy that has an acceptable performance with appreciable reduction in the magnitudes of harmonic distortion obtained during modulation which leads to optimum performance index.

(Keywords: space vector modulation, third harmonic modulation, induction motor drive)

INTRODUCTION

The production of AC voltage having instantaneous average value varying below or above the input DC voltage is among the basic requirements for most pulse-width modulated (PWM) inverters in various domestic and industrial drive applications such as uninterruptible power supply (UPS), static frequency changes, variable speed drives and distributed power generators. This requirement suffice it to say, is achieved with the traditional voltage source inverter which is been modulated using either a space vector or a third harmonic injected modulation.

Space vector pulse width modulation (SVPWM) is a modulation technique that involves the generation of a reference vector V_{ref} representing a three phase sinusoidal voltage realized by switching between two nearest active vectors and one zero vector switching sequence of a given power converter [1]. This modulation technique is been compared here with a third harmonic injected modulation at modulation index of 0.8 for 3, 5 and 7-level diode clamped converter (DCC). The results obtained were used to drive a 10 HP, 400volts 50Hz induction motor.

Switching On-Time of the Two Active and Zero Vectors of SVPWM Based DCC

The Switching on-time determination of a multilevel inverter applying Space Vector is realized by the method adopted by Gupta and Khambadkone presented in the flow chart of Figure 1 and this formed the basis of dwell time calculation for the Simulink models representing SVPWM of multi-level diode clamped converter [2]. The magnitude of the reference vector and its corresponding angle was realized using Simulink block models.

The equations used in the modeling of a three phase, SVPWM of multi-level converter with respect to the reference vector angle and magnitudes are presented below [3]:

$$V_{AN} = \frac{1}{\sqrt{3}} \times V_{LL} \times \cos \omega t \qquad (1)$$

$$V_{BN} = \frac{1}{\sqrt{3}} \times V_{LL} \times \cos\left(wt - \frac{2\pi}{3}\right) \qquad (2)$$

$$V_{CN} = \frac{1}{\sqrt{3}} \times V_{LL} \times \cos\left(wt - \frac{4\pi}{3}\right) \quad (3)$$

The space vector voltage is given by:

$$V_s = \frac{2}{3} \times (V_{AN} + aV_{BN} + a^2V_{CN}) \quad (4)$$

Where $a = \cos 120^0 + j \sin 120^0$ and $a^2 = \cos 240^0 + j \sin 240^0$. For a balanced three phase system, the magnitude of the output voltages and their corresponding frequency must be equal. Therefore substituting the values of "**a**" and $\mathbf{a^2}$ and with only the corresponding voltage magnitude of the above three phase voltages into (4) produces Equation (5) as shown:

$$V_s = \frac{2}{3} \times (|V| + j|V| \sin 120^0 + |V| \cos 240^0 + j|V| \sin 240^0) \quad (5)$$

Re-arranging (5) into real and imaginary paths produces (6) as shown below:

$$V_s = \frac{2}{3}(|V| + |V| \cos 120^0 + |V| \cos 240^0 + j(|V| \sin 120^0 + |V| \sin 240^0)) \quad (6)$$

Since d-q voltages are orthogonal (right-angled) to each other. Then (6) aligned in the d-q plane produces (7) and (8), respectively:

$$V_d = \frac{2}{3}(|V| + |V| \cos 120^0 + |V| cos 240^0) \quad (7)$$

$$V_q = \frac{2}{3}(|V| \sin 120^0 + |V| sin 240^0) \quad (8)$$

Equations (7) and (8) formed the basic equation model for the generation of the reference angle and magnitude of reference vector which is achieved by using the Cartesian to polar block got from transformation block in the Simulink extras contained in the Simulink sub-library.

The injected 3rd order harmonic has the following equations for its modeling: The three phase reference voltage equation and the injected 3rd harmonic modulating equation shown below [3]. The third harmonic injected reference signal as well as the 3, 5, and 7-level carrier signal were all realized using Simulink model block.

Similarly, the 3, 5 and 7-level DCC were all built in Simulink environment and there results were presented in the paper.

$$V_a = mi \times \cos \omega t \quad (9)$$

$$V_{a3} = \frac{-mi}{6} \times \cos 3\omega t \quad (10)$$

$$V_b = mi \times \cos\left(\omega t - \frac{2\pi}{3}\right) \quad (11)$$

$$V_{b3} = \frac{-mi}{6} \times \cos 3\omega t \quad (12)$$

$$V_c = mi \times \cos\left(\omega t - \frac{4\pi}{3}\right) \quad (13)$$

$$V_{c3} = \frac{-mi}{6} \times \cos 3\omega t \quad (14)$$

Comparative Analyses between SVPWM and Third Harmonic Injected Modulation

In [4], the technical report showed that when a carrier-based modulation is injected with a third harmonic; the result obtained from this modulation technique produces the same result as that obtained using space vector pulse width modulation strategy.

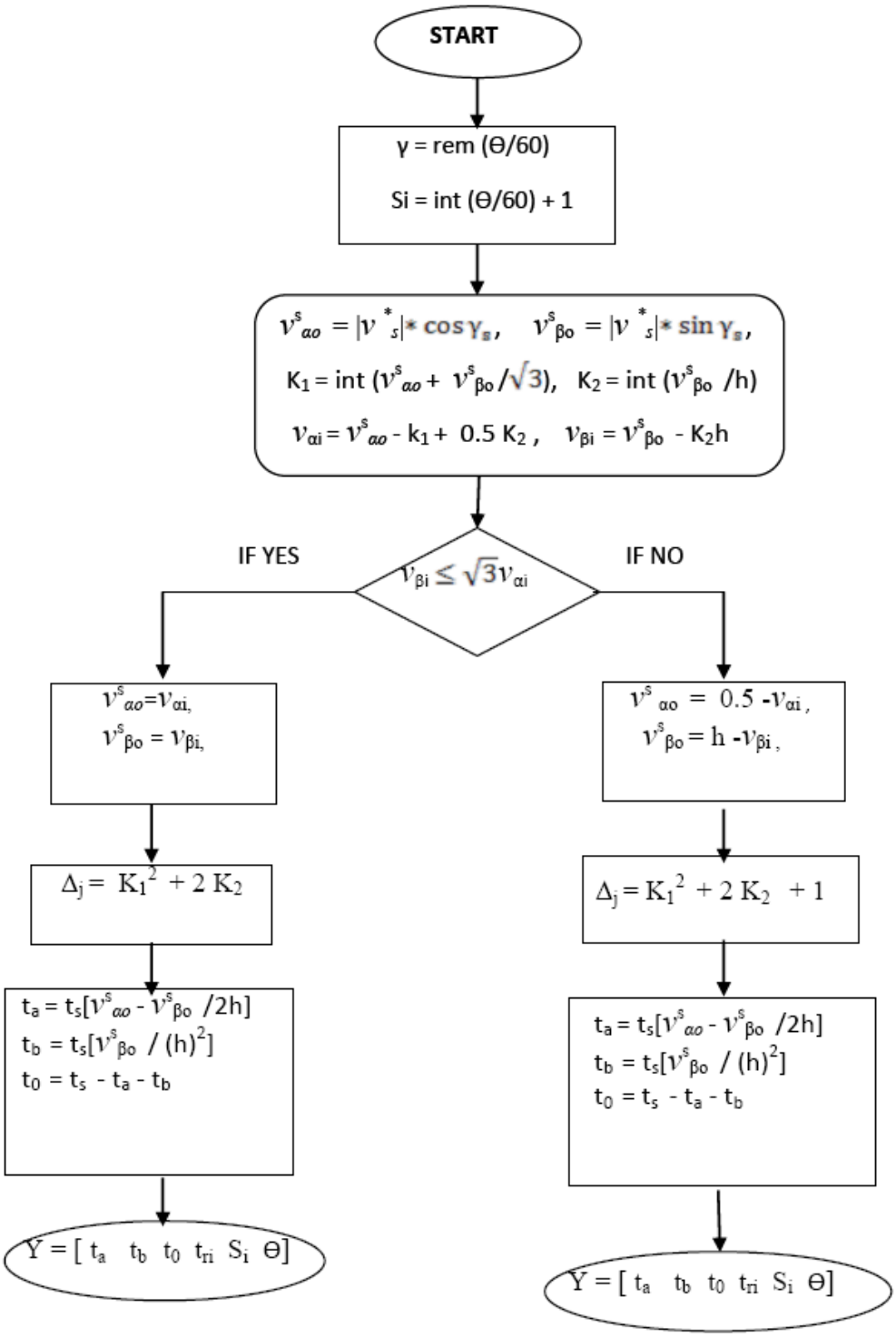

Figure 1: Flow-Chart for Sector Determination and Switching On-Time of SVPWM.

The result of this analogy is reflected in simulation results presented in Figures 2-7, respectively.

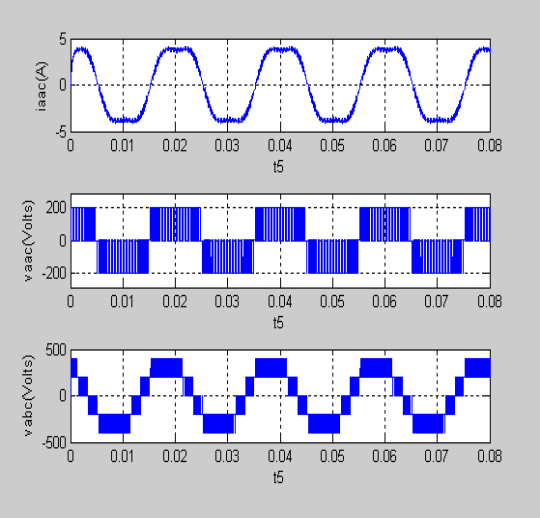

Figure 2: 3-level DCC Wave form at 0.8 Modulation Index using 3rd Harmonic Injected Modulation Technique.

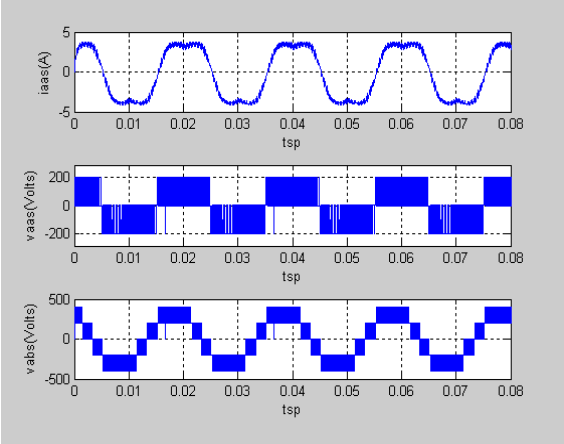

Figure 3: 3-level DCC Waveform at 0.8 Modulation Index using SVPWM Technique.

Simulink Modelling of a Three Level DCC Fed Induction Machine

Induction machine is the most widely used machinery in various industries this is because of its robustness, low cost, high efficiency and good self-starting capability.

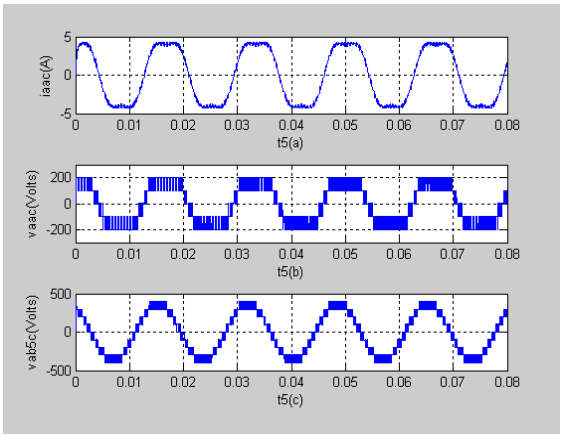

Figure 4: 5-level DCC Waveform at 0.8 Modulation Index using 3rd Harmonic Injected Modulation Technique.

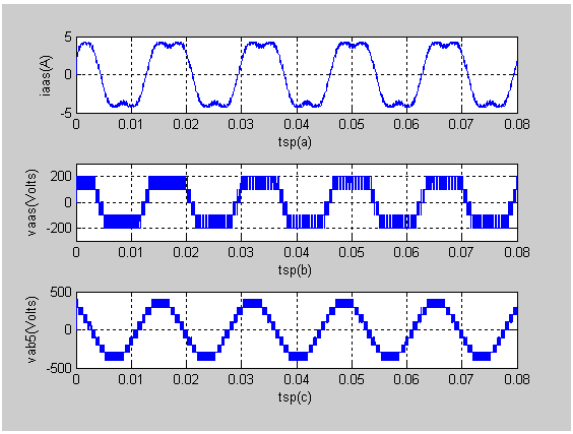

Figure 5: 5-level DCC Waveform at 0.8 Modulation Index Using SVPWM Technique

Despite these good features, the induction motor still has limitation such as not having a true constant- speed due to variation in slip at different frequencies below or above the rated (fundamental) value [5].

Therefore, experts through technical reports proved that this inherent limitation can be corrected with the aid of a voltage source inverter when used as the induction motor driving source at constant supply frequency [5].

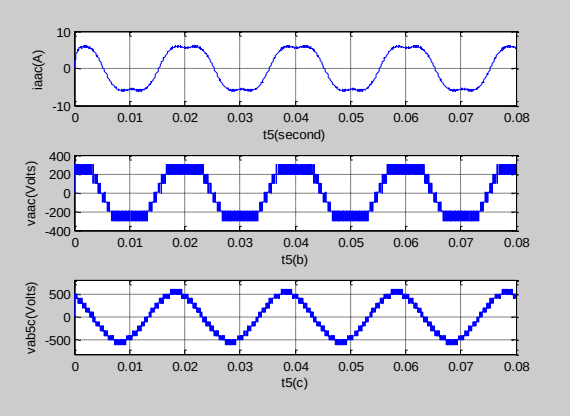

Figure 6: 7-level DCC Waveform at 0.8 Modulation Index using 3rd Harmonic Injected Modulation Technique.

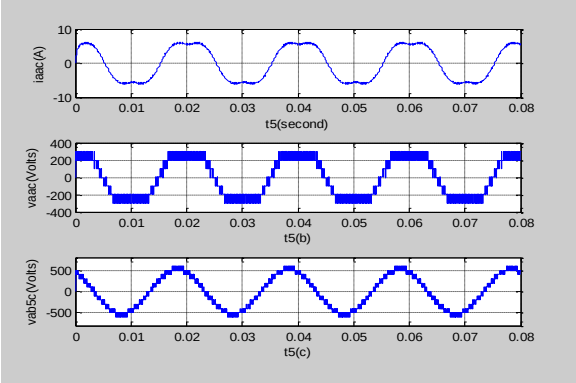

Figure 7: 7-level DCC Waveform at 0.8 Modulation Index using SVPWM Technique.

The voltage equations of the induction motor which give rise to the dynamic equivalent circuit of the squirrel cage induction motor shown in Figure 8 is given by (15) – (22) with the zero sequence voltage neglected [6]. In this analysis, the stator voltages of the machine are been fed by the three phase, three level voltage source inverter as shown in Figures 9 and 10.

$$V_{qs} = r_s i_{qs} + \omega\lambda_{ds} + P\lambda_{qs} \quad (15)$$

$$V_{ds} = r_s i_{ds} - \omega\lambda_{qs} + P\lambda_{ds} \quad (16)$$

$$V'_{qr} = r'_r i'_{qr} + (\omega - \omega_r)\lambda'_{dr} + P\lambda'_{qr} \quad (17)$$

$$V'_{dr} = r'_r i'_{dr} - (\omega - \omega_r)\lambda'_{qr} + P\lambda'_{dr} \quad (18)$$

Where:

$$\lambda_{qs} = L_{ls} i_{qs} + L_m(i_{qs} + i'_{qr}) \quad (19)$$

$$\lambda_{ds} = L_{ls} i_{ds} + L_m(i_{ds} + i'_{dr}) \quad (20)$$

$$\lambda'_{qr} = L'_{lr} i'_{qr} + L_m(i_{qs} + i'_{qr}) \quad (21)$$

$$\lambda'_{dr} = L'_{lr} i'_{dr} + L_m(i_{ds} + i'_{dr}) \quad (22)$$

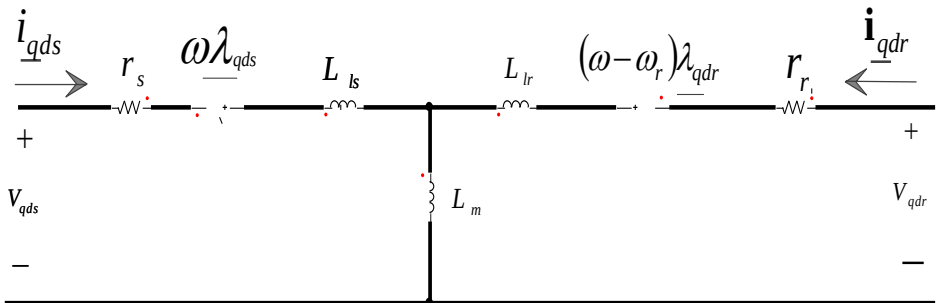

Figure 8: Dynamic Equivalent Circuit of a Squirrel Cage Induction Motor in Synchronous Reference Frame.

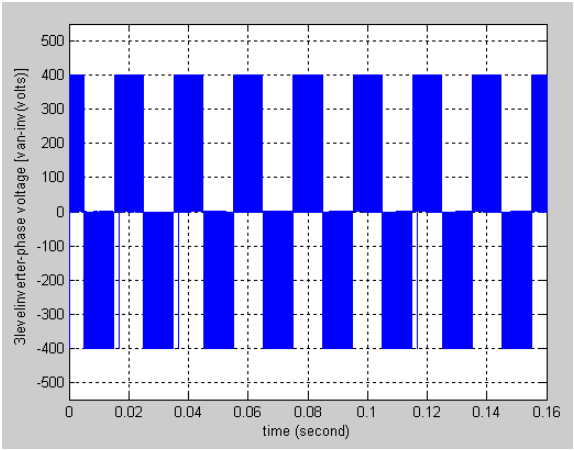

Figure 9: 3-Level DCC Phase Voltage.

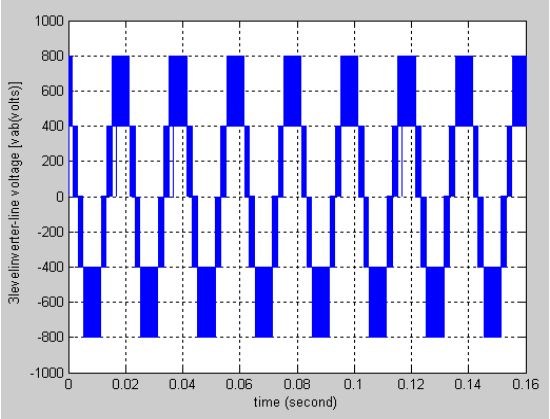

Figure 10: 3-level DCC Line Voltage.

In this section, a three level diode clamped converter was modulated using a space vector and third harmonic injected modulation technique. The modulated three level DCC was used here to drive a 10hp, 400V, 50Hz induction motor. Total harmonic distortions for the respective motor parameters were determined using the total harmonic distortion block (THD) obtained from the discreet block under the Simulink extra contained in the Simulink sub-library. The actual model for the simulation of a 3-level voltage source inverter fed induction motor using space vector control mechanism was also implemented in Simulink. An interconnection between the inverter and the induction motor is a filter that attenuates any undesirable harmonics infiltrating into the machine. The motor electrical inputs such as the stator currents for the three phase as well as the voltages for the d-q axes with a corresponding output torque and motor speed were obtained using the bus-selector. The induction machine model was obtained from the SimPowerSystems under simulink sub-library.

Results of a Three-Level DCC Fed Induction Motor

The simulation results for the 3-level voltage source inverter fed induction motor as explained above were shown in Figures 9-13. Simulation parameters used are as follows: supply voltage V_s = 400V, stator resistance R_s = 0.4Ω, rotor resistance R_r = 0.2Ω, stator and rotor leakage inductances L_{Ls} = L_{Lr} = 0.0048H, magnetizing inductance L_m = 95.5mH. Motor inertia J = 0.25 Kgm^2, coefficient of frictional factor B= 0.001N.M.S. Nominal Machine powe = 10 HP (7.5kW), number of poles = 4, operating

frequency = 50Hz, synchronous speed = 1500rpm.

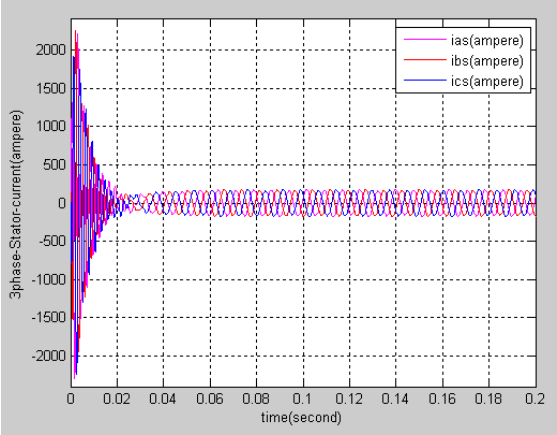

Figure 11: 3-Phase Currents of 3-level DCC.

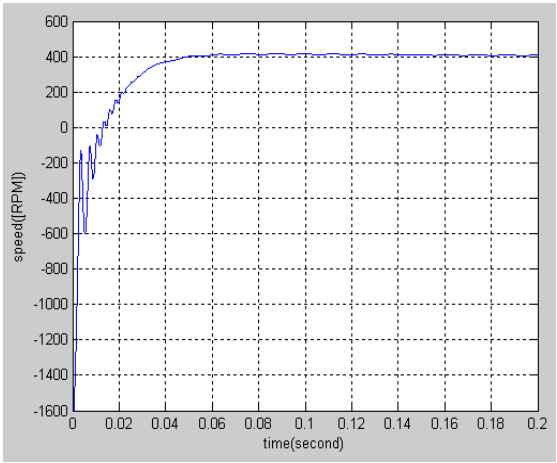

Figure 12: 3-Phase Induction Motor Variable Speed.

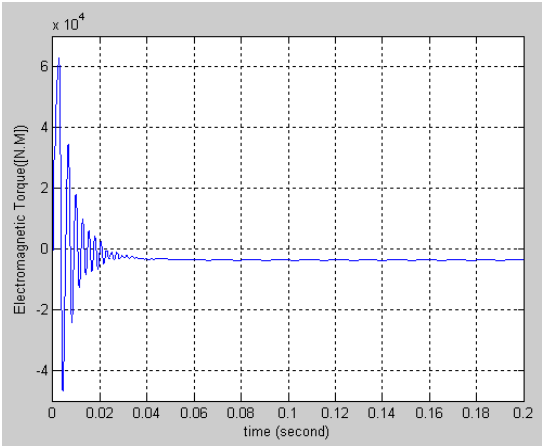

Figure 13: Electromagnetic Torque of the Induction Motor.

The results obtained from the above machine simulation showed that the induction motor produced a high running performance during starting with a high starting current corresponding to a low rotor resistance of R_r = 0.2Ω, and low rotor leakage inductance of L_{Lr} = 0.0048H and a high starting torque. It was observed that during starting the motor speed rose from -1500rpm and attained a steady state speed of 420rpm after 0.06second. A strong oscillation of the electromagnetic torque was observed during the starting period of the motor before a steady state value was attained at 0.06second with a corresponding value of -2500Nm. This positive value of speed and the negative value of the torque at steady state indicates a regenerative braking characteristics of the induction motor.

Table 1: THD Values for the 3-Level DCC Fed Induction Motor at 0.8 Modulation Index

THD for 3level DCC fed induction motor with space vector pulse width modulation at 0.8 modulation index	THD for 3level DCC fed induction motor with 3rd Harmonic injected modulation at 0.8 modulation index
Induction motor speed = 10.21%	Induction motor speed = 17.87%
Electromagnetic Torque = 7.82%	Electromagnetic Torque = 13.56%

CONCLUSION

Analysis of the results presented in Figures 2 - 7 confirmed the postulations carried out by D.G Holmes and T.A. Lipo implying that at a modulation index of 0.8, a carrier-based modulation injected with a third harmonic produces the same result with space vector pulse-width modulation at the same modulation index.

The results obtained in Figures 9-13 showed that the induction motor produced a high running performance during starting with a high starting current corresponding to a low rotor resistance and leakage inductance.

During starting, it was observed that the motor speed rose from -1500rpm and attained a steady state speed of 420rpm after 0.06second. A strong oscillation of the electromagnetic torque was observed during this starting period before a steady state value was attained at 0.06 second

with a corresponding torque of -2500NM. This positive value of speed and negative value of torque at steady state indicates a regenerative braking characteristic of the induction motor.

Table 1 showed that a reduced value of percentage total harmonic distortion for the motor speed and torque is achieved with the aid of a space vector pulse width modulation and thus should be adopted in the induction motor drive strategy to avoid undue heat losses associated with harmonic

REFERENCES

1. Kanchan, R.S. and M.R. Mohapatara. 1996. "Space Vector PWM Signal Generator for Multi-Level Inverters". VPEC Seminar. 221-233

2. Gupta, A.K. and A.M. Khambadkone. 2005, "A General Space Vector PWM Algorithm for a Multi-Level Inverter, Including Operation in Over Modulation Range''. *Proc. IEEE IEMDC*.1437-1444.

3. Holmes, D.G. and T.A. Lipo. 2003. "Pulse Width Modulation for Power Converters Principles and Practice". IEEE Press / Wiley- Interscience: New York, NY.

4. Holmes, D.G. 2000. "The General Relationship between Regular- Sampled Pulse Width Modulation and Space Vector Modulation for Hard Switched Converters". *Conf. Rec. IEEE- IAS Annual Meeting*. 2482-2488.

5. Richard, M.C. 1995. *Electric Drives and their Control*. Oxford University Press: New York, NY.

6. Ong, C.M. 1998. *Dynamic Simulation of Electric Machinery Using Matlab/Simulink*. Prentice Hall PTR: Upper Saddle River, NJ.

SUGGESTED CITATION

Omeje, C.O., D.B. Nnadi, and C.I. Odeh. 2012. "Comparative Analysis of Space Vector Pulse-Width Modulation and Third Harmonic Injected Modulation on Industrial Drives". *Pacific Journal of Science and Technology*. 13(1):12-19.

Pacific Journal of Science and Technology